Inorg. Chem. **2009**, *48*, 4435−4444

Redox-Regulated Inhibition of T7 RNA Polymerase via Establishment of Disulfide Linkages by Substituted Dppz Dirhodium(II,II) Complexes

J. Dafhne Aguirre,[†] Helen T. Chifotides,[†] Alfredo M. Angeles-Boza,[†] Abdellatif Chouai,[†] Claudia Turro,*[,‡] and Kim R. Dunbar*[,†]

Department of Chemistry, Texas A&M University, College Station, Texas 77843, and Department of Chemistry, The Ohio State University, Columbus, Ohio 43210

Received January 26, 2009

The series of dirhodium(II) complexes *cis*-$[Rh_2(O_2CCH_3)_2(R_1R_2dppz)_2]^{2+}$ **1**−**6** ($R_1 = R_2 =$ H, MeO, Me, Cl, NO_2 for **1**−**4**, **6**, respectively, and $R_1 =$ H, $R_2 =$ CN for **5**), coordinated to R_1R_2dppz ligands with electron-donating or -withdrawing substituents at positions 7,8 of dppz (dppz = dipyrido[3,2-*a*:2′,3′-*c*]phenazine), were synthesized and their effect on the transcription process in vitro was monitored. Complexes **1**−**6** are easily reduced, readily oxidize cysteine, and engage in redox-based reactions with T7-RNA Polymerase (T7-RNAP), which contains accessible thiol groups. Transcription is inhibited in vitro by **1**−**6** via formation of intra- and inter-T7-RNAP disulfide bonds that affect the enzyme critical sulfhydryl cysteine groups. The progressively increasing electron-withdrawing character of the dppz substituents (MeO < Me < H < Cl < CN < NO_2) gives rise to the order **2** < **3** < **1** < **4** < **5** < **6** for the measured IC_{50} values of **1**−**6**. The ease of reduction for **1**−**6** is consistent with the energies of the dppz-centered lowest unoccupied molecular orbitals (LUMOs), which decrease with the electron-withdrawing character of the dppz substituents. The ligand-centered reductions for **1**−**6** are supported by electron paramagnetic resonance (EPR) studies which support the conclusion that reduction of **1**−**6** leads to the formation of dppz centered radicals $[Rh_2(O_2CCH_3)_2(R_1R_2dppz)_2]^{\bullet+}$ with isotropic *g* values ∼2.003 which are essentially identical to the reported value for the free radical dppz anions. The EPR results are corroborated by density functional theory (DFT) calculations, which indicate that the complexes contain dppz-based LUMOs primarily phenazine (phz) in character; the unpaired electron is completely delocalized in the phenazine orbitals in **4**−**6**. The low IC_{50} values for **1**−**6** lend further support to the fact that they exhibit redox-based activity with the enzyme and lead to the conclusion that the complexes constitute a sensitive redox-regulated series of T7-RNAP inhibitors with the potential to control or inhibit other important biochemical processes.

Introduction

In recent years, dirhodium complexes with metal−metal bonds[1] have attracted much attention because of their considerable carcinostatic activity against various tumor cell lines[2−9] and their interactions with DNA.[10] Although the mechanism(s) of action for dirhodium antitumor active complexes remains to be elucidated, it is well established

* To whom correspondence should be addressed. E-mail: dunbar@mail.chem.tamu.edu (K.R.D.), turro@chemistry.ohio-state.edu. (C.T.).
† Texas A&M University.
‡ The Ohio State University.

(1) Chifotides, H. T.; Dunbar, K. R. Rhodium Compounds. In *Multiple Bonds Between Metal Atoms*, 3rd ed; Cotton, F. A., Murillo, C., Walton, R. A., Eds.; Springer-Science and Business Media, Inc.: New York, 2005; Chapter 12, pp 465−589.
(2) Hughes, R. G.; Bear, J. L.; Kimball, A. P. *Proc. Am. Assoc. Cancer Res.* **1972**, *13*, 120.
(3) Howard, R. A.; Kimball, A. P.; Bear, J. L. *Cancer Res.* **1979**, *39*, 2568–2573.
(4) Erck, A.; Rainen, L.; Whileyman, J.; Chang, I.-M.; Kimball, A. P.; Bear, J. L. *Proc. Soc. Exp. Biol. Med.* **1974**, *145*, 1278–1283.
(5) Bear, J. L.; Gray, H. B., Jr.; Rainen, L.; Chang, I. M.; Howard, R.; Serio, G.; Kimball, A. P. *Cancer Chemother. Rep.* **1975**, *59*, 611–620.
(6) Howard, R. A.; Sherwood, E.; Erck, A.; Kimball, A. P.; Bear, J. L. *J. Med. Chem.* **1977**, *20*, 943–946.
(7) Zyngier, S.; Kimura, E.; Najjar, R. *Braz. J. Med. Biol. Res.* **1989**, *22*, 397–401.
(8) Bear, J. L. *Precious Metals 1985: Proceedings of the Ninth International Precious Metals Conference*; Zysk, E. D.; Bonucci, J. A., Eds.; Int. Precious Metals: Allentown, PA, 1986; p 337.
(9) De Souza, A. R.; Coelho, E. P.; Zyngier, S. B. *Eur. J. Med. Chem.* **2006**, *41*, 1214–1216.
(10) Chifotides, H. T.; Dunbar, K. R. *Acc. Chem. Res.* **2005**, *38*, 146–156 and references therein.

10.1021/ic900164j CCC: $40.75
Published on Web 04/15/2009

that purine nucleobases,[11−17] nucleos(t)ides,[18−22] as well as single-[23−26] and double-stranded DNA[27] bind to dirhodium complexes. Dirhodium compounds are also known to be potent inhibitors of transcription[28−30] and DNA replication[31] in vitro. It appears that several dirhodium complexes achieve transcription inhibition in vitro by binding to the RNA polymerase,[29] whereas cisplatin interferes with transcription primarily by forming 1,2-d(GpG) intrastrand cross-links with DNA, the result of which is the hijacking of various proteins to the platinated sites and disruption of their normal function.[32−34] It has been documented that apart from transcription inhibition by modification/damage to the DNA,[35−37] suppression of transcription can arise from drug binding to the active site of RNA Polymerase, from blocking of the DNA/RNA channel,[38,39] or from targeting of transcription factors.[40]

The bacteriophage T7-RNA Polymerase (T7-RNAP) system is a relatively simple enzyme that carries out the transcription cycle in an identical manner to that of bacterial and eukaryotic RNAPs;[41,42] the single-subunit T7-RNAP protein (99 kDa) is capable of initiation, elongation, and termination. The mechanistic and kinetic aspects of the process have been extensively investigated and are well understood.[43−49] In particular, the structures of various key intermediates provide a detailed picture of the enzyme's action.[44−48] The initial binding of the enzyme to the promoter sequence of the template DNA to form the initiation complex (IC)[44−47,50,51] is followed by a number of abortive cycles that result in the production of short mRNA transcripts that range from 2 to ∼6 bases.[44−47,52] At the stage where the transcript reaches a length of ∼7−8 bases, a transition takes place to the elongation complex (EC), which ultimately produces the long mRNA transcript.[44−47,50,52] Crystal structures have been previously determined for the T7-RNAP protein,[53] the complex with a 17-base-pair DNA promoter,[54] as well as the IC[55] and the ECs.[56,57] Further studies have shown that significant structural reorganization occurs during the transition from the IC to the EC.[48,58,59]

The T7-RNAP contains 12 cysteine residues[60] in the free sulfhydryl form as evidenced from titrations of the urea-denatured protein with 5,5′-dithiobis(nitrobenzoic acid) DTNB (Ellman's reagent).[61] As indicated in previous reports, one or more titrable sulfhydryl groups are important for the activity of the enzyme: reactions performed with active T7-RNAP and DTNB[59] or [^{14}C]iodoacetamide[61] over several days revealed a stoichiometry of 2 cysteine (Cys) residues per native wild type T7-RNAP. Moreover, the addition of

(11) Pneumatikakis, G.; Hadjiliadis, N. *J. Chem. Soc., Dalton Trans.* **1979**, 596–599.
(12) Rubin, J. R.; Haromy, T. P. *Acta Crystallogr.* **1991**, *C47*, 1712–1714.
(13) Aoki, K.; Salam, Md. A. *Inorg. Chim. Acta* **2002**, *339*, 427–437.
(14) Dunbar, K. R.; Matonic, J. H.; Saharan, V. P.; Crawford, C. A.; Christou, G. *J. Am. Chem. Soc.* **1994**, *116*, 2201–2202.
(15) Crawford, C. A.; Day, E. F.; Saharan, V. P.; Folting, K.; Huffman, J. C.; Dunbar, K. R.; Christou, G. *Chem. Commun.* **1996**, 1113–1114.
(16) Angeles-Boza, A. M.; Chifotides, H. T.; Aguirre, J. D.; Chouai, A.; Fu, P. K.-L.; Dunbar, K. R.; Turro, C. *J. Med. Chem.* **2006**, *49*, 6841–6847.
(17) Deubel, D. V.; Chifotides, H. T. *Chem. Commun.* **2007**, 3438–3440.
(18) Chifotides, H. T.; Koshlap, K. M.; Pérez, L. M.; Dunbar, K. R. *J. Am. Chem. Soc.* **2003**, *125*, 10703–10713.
(19) Chifotides, H. T.; Koshlap, K. M.; Pérez, L. M.; Dunbar, K. R. *J. Am. Chem. Soc.* **2003**, *125*, 10714–10724.
(20) Chifotides, H. T.; Dunbar, K. R. *Chem.—Eur. J.* **2006**, *12*, 6458–6468.
(21) Chifotides, H. T.; Dunbar, K. R. *J. Am. Chem. Soc.* **2007**, *129*, 12480–12490.
(22) Chifotides, H. T.; Dunbar, K. R. *Chem.—Eur. J.* **2008**, *14*, 9902–9913.
(23) Chifotides, H. T.; Koomen, J. M.; Kang, M.; Tichy, S. E.; Dunbar, K. R.; Russell, D. H. *Inorg. Chem.* **2004**, *43*, 6177–6187.
(24) Asara, J. M.; Hess, J. S.; Lozada, E.; Dunbar, K. R.; Allison, J. *J. Am. Chem. Soc.* **2000**, *122*, 8–13.
(25) Chifotides, H. T.; Dunbar, K. R. *Angew. Chem., Int. Ed.* **2006**, *45*, 6148–6151.
(26) Kang, M.; Chifotides, H. T.; Dunbar, K. R. *Biochemistry* **2008**, *47*, 2265–2276.
(27) Dunham, S. U.; Chifotides, H. T.; Mikulski, S.; Burr, A. E.; Dunbar, K. R. *Biochemistry* **2005**, *44*, 996–1003.
(28) Sorasaenee, K.; Fu, P. K.-L.; Angeles-Boza, A. M.; Dunbar, K. R.; Turro, C. *Inorg. Chem.* **2003**, *42*, 1267–1271.
(29) Chifotides, H. T.; Fu, P. K.-L.; Dunbar, K. R.; Turro, C. *Inorg. Chem.* **2004**, *43*, 1175–1183.
(30) Aguirre, J. D.; Lutterman, D. A.; Angeles-Boza, A. M.; Dunbar, K. R.; Turro, C. *Inorg. Chem.* **2007**, *46*, 7494–7502.
(31) Dale, L. D.; Dyson, T. M.; Tocher, D. A.; Tocher, J. H.; Edwards, D. I. *Anti-Cancer Drug Des.* **1989**, *4*, 295–302.
(32) Zamble, D. B.; Lippard, S. J. In *Cisplatin: Chemistry and Biochemistry of a Leading Anticancer Drug*; Lippert, B., Ed.; Wiley-VCH: Weinheim, 1999; pp 73−110.
(33) Barnes, K. R.; Lippard, S. J. *Met. Ions Biol. Syst.* **2004**, *42*, 143–177.
(34) Jung, Y.; Lippard, S. J. *J. Biol. Chem.* **2003**, *278*, 52084–52092.
(35) Imamichi, T.; Murphy, M. A.; Adelsberger, J. W.; Yang, J.; Watkins, C. M.; Berg, S. C. B.; Michael, W. L.; Richard, A.; Guo, J.; Levin, J. G.; Lane, H. C. *J. Virol.* **2003**, *77*, 1011–1020.
(36) Marin, S.; Mansilla, S.; Garcia-Reyero, N.; Rojas, M.; Portugal, J.; Pina, B. *Biochem. J.* **2002**, *368*, 131–136.
(37) Portugal, J.; Martin, B.; Vaquero, A.; Ferrer, N.; Villamarin, S.; Priebe, W. *Curr. Med. Chem.* **2001**, *8*, 1–8.
(38) Luo, G.; Lewis, R. A. *Biochem. Pharmacol.* **1992**, *44*, 2251–2258.
(39) Campbell, E. A.; Korzheva, N.; Mustaev, A.; Murakami, K.; Nair, S.; Goldfarb, A.; Darst, S. A. *Cell* **2001**, *104*, 901–912.
(40) Chao, S.-H.; Price, D. H. *J. Biol. Chem.* **2001**, *276*, 31793–31799.
(41) Cheetham, G. M. T.; Steitz, T. A. *Curr. Opinion Struct. Biol.* **2000**, *10*, 117–123.
(42) McAllister, W. T. *Cell. Mol. Biol. Res.* **1993**, *39*, 385–391.
(43) Sousa, R.; Mukherjee, S. *Prog. Nucleic Acid Res. Mol. Biol.* **2003**, *73*, 1–41.
(44) Cheetham, G. M. T.; Steitz, T. A. *Curr. Opin. Struct. Biol.* **2000**, *10*, 117–123.
(45) Doublié, S.; Tabor, S.; Long, A. M.; Richardson, C. C.; Ellengerger, T. *Nature (London)* **1998**, *391*, 251–258.
(46) McAllister, W. T. *Nucl. Acids Mol. Biol.* **1997**, *11*, 15–25.
(47) Ujvári, A.; Martin, C. T. *J. Mol. Biol.* **1997**, *273*, 775–781.
(48) Nayak, D.; Siller, S.; Guo, Q.; Sousa, R. *J. Mol. Biol.* **2008**, *376*, 541–553.
(49) Termiakov, D.; Mentesana, P. E.; Ma, K.; Mustaev, A.; Borukhov, S.; McAllister, W. T. *Proc. Natl. Acad. Sci. U.S.A.* **2000**, *97*, 14109–14114.
(50) Kochetkov, S. N.; Rusakova, E. E.; Tunitskaya, V. L. *FEBS Lett.* **1998**, *440*, 264–267.
(51) Guo, Q.; Nayak, D.; Brieba, L. G.; Sousa, R. *J. Mol. Biol.* **2005**, *353*, 256–270.
(52) Jia, Y.; Patel, S. S. *Biochemistry* **1997**, *36*, 4223–4232.
(53) Sousa, R.; Chung, Y. J.; Rose, J. P.; Wang, B. C. *Nature (London)* **1993**, *364*, 593–599.
(54) Cheetham, G. M. T.; Jeruzalmi, D.; Steitz, T. A. *Nature (London)* **1999**, *399*, 80–83.
(55) Cheetham, G. M. T.; Steitz, T. A. *Science* **1999**, *286*, 2305–2309.
(56) Tahirov, T. H.; Temiakov, D.; Anikin, M.; Patlan, V.; McAllister, W. T.; Vassylyev, D. G.; Yokoyama, S. *Nature (London)* **2002**, *420*, 43–50.
(57) Yin, Y. W.; Steitz, T. A. *Science* **2002**, *298*, 1387–1395.
(58) Ma, K.; Temiakov, D.; Jiang, M.; Anikin, M.; McAllister, W. T. *J. Biol. Chem.* **2002**, *277*, 43206–43215.
(59) Mukherjee, S.; Brieba, L. G.; Sousa, R. *Cell* **2002**, *110*, 81–91.
(60) Moffatt, B. A.; Dunn, J. J.; Studier, F. W. *J. Mol. Biol.* **1984**, *173*, 265–269.
(61) King, G. C.; Martin, C. T.; Pham, T. T.; Coleman, J. E. *Biochemistry* **1986**, *25*, 36–40.

Chart 1. Structure and Numbering of Dipyrido[3,2-*a*:2′,3′-*c*]phenazine (dppz)

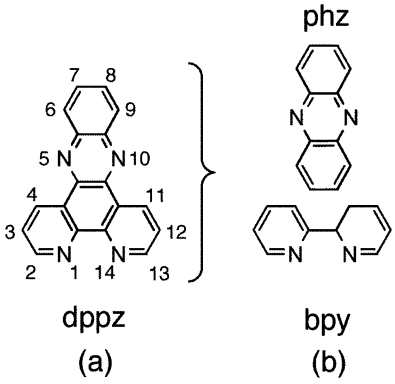

10^{-5} M *p*-hydroxymercuribenzoate (sulfhydryl binding agent) to the transcription reaction abolishes all enzyme activity,[62] and T7-RNAP is inactivated within minutes or 5 h by reaction with 10^{-3} M DTNB[63] or 10^{-2} M [^{14}C]iodoacetamide,[63,64] respectively. In particular, peptide analysis following digestion of the trypsin digested T7-RNAP after reaction with 10−20 fold excess of [^{14}C]iodoacetamide showed Cys-347 and Cys-723 to be the significantly iodoacetamide-reactive Cys residues.[61] Exposure of the enzyme to other oxidizing conditions[65] or storage in the absence of sulfhydryl reducing agents, for example, mercaptoethanol or dithiothreitol (DTT), results in considerably reduced enzyme activity.[62] It is notable that substitution of 7 of the 12 cysteine with serine residues can be made without large reduction in the enzyme activity, but mutation of the remaining 5 cysteine residues results in loss of the T7-RNAP activity.[59]

In recent years, dipyrido[3,2-*a*:2′,3′-*c*]phenazine (dppz; Chart 1a) complexes have received appreciable attention because of their ability to intercalate DNA.[66,67] Dirhodium complexes equipped with dppz ligands have been shown to photocleave DNA and are considered to be promising candidates for photodynamic therapy.[68−70] The mono dppz derivative $[Rh_2(O_2CCH_3)_2(dppz)(\eta^1\text{-}O_2CCH_3)(CH_3OH)]^+$ was found to intercalate between the DNA bases, in contrast to $[Rh_2(O_2CCH_3)_2(dppz)_2]^{2+}$, which is not a DNA intercalator, but nevertheless exhibits a significantly higher photocytotoxicity than the former dirhodium complex.[68] Structurally dppz can be considered to consist of a 2,2′-bipyridine (bpy) chelate with a phenazine (phz) unit appended to it (Chart 1b). Dppz exhibits features of *a*-diimine chelate ligands such as bpy or 1,10-phenanthroline (phen) whose chemistry with various dirhodium complexes has already been extensively studied.[71] Indeed, inhibition of transcription by binding of *cis*-$[Rh_2(O_2CCH_3)_2(phen)_2]^{2+}$ to T7-RNAP has been reported.[28] The chemistry of the dppz ligand is of further interest in the context of biological reactions because it possesses low lying unoccupied phz-based molecular orbitals (LUMO b_1(phz))[72−74] the presence of which promotes reduction of its complexes leading to the formation of radical anions with the charge located on the phz part of the ligand.[75,76]

Chart 2. Dirhodium Complexes *cis*-$[Rh_2(O_2CCH_3)_2(R_1R_2dppz)_2]^{2+}$

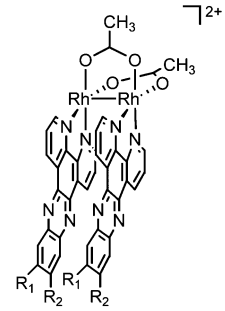

$R_1 = R_2 = H$, **1**
$R_1 = R_2 = MeO$, **2**
$R_1 = R_2 = Me$, **3**
$R_1 = R_2 = Cl$, **4**
$R_1 = H$, $R_2 = CN$, **5**
$R_1 = R_2 = NO_2$, **6**

In the present work, a series of cationic dirhodium complexes **1**−**6** possessing substituted dppz ligands with electron-donating or -withdrawing substituents, namely, *cis*-$[Rh_2(O_2CCH_3)_2(R_1R_2dppz)_2]^{2+}$ (R_1R_2dppz = substituted dppz; Chart 2), were prepared and their effect on the transcription process in vitro was monitored. Spectroscopic characterizations of the dirhodium complexes, as well as DFT calculations that corroborate the observed activity, were undertaken. The electron-withdrawing or -donating substituents on the dppz ligands (at sites 7,8 of the phz fragment) of each complex affect the ease of reduction, hence their redox-based reactions with the cysteine groups of T7-RNAP and the degree of transcription inhibition. To our knowledge, this is the first report of transcription inhibition effected by redox reactions of metal complexes. To this effect, a series of catalytic Ru(II) complexes, which are cytotoxic to cancer cells by inducing redox chemistry with glutathione, were recently reported.[77]

(62) Chamberlin, M.; Ring, J. *J. Biol. Chem.* **1973**, *248*, 2235–2241.
(63) Oakley, J. L.; Pascale, J. L.; Coleman, J. E. *Biochemistry* **1975**, *14*, 4684–4691.
(64) Giedroc, D. P.; Keating, K. M.; Martin, C. T.; Williams, K. R.; Coleman, J. E. *J. Inorg. Biochem.* **1986**, *28*, 155–169.
(65) Esposito, E. A.; Martin, C. T. *J. Biol. Chem.* **2004**, *279*, 44270–44276.
(66) Holmlin, R. E.; Yao, J. A.; Barton, J. K. *Inorg. Chem.* **1999**, *38*, 174–189.
(67) Shao, F.; Barton, J. K. *J. Am. Chem. Soc.* **2007**, *129*, 14733–14738.
(68) Angeles-Boza, A. M.; Bradley, P. M.; Fu, P. K. L.; Wicke, S. E.; Bacsa, J.; Dunbar, K. R.; Turro, C. *Inorg. Chem.* **2004**, *43*, 8510–8519.
(69) Angeles-Boza, A. M.; Bradley, P. M.; Fu, P. K. L.; Shatruk, M.; Hilfiger, M. G.; Dunbar, K. R.; Turro, C. *Inorg. Chem.* **2005**, *44*, 7262–7264.
(70) Bradley, P. M.; Angeles-Boza, A. M.; Dunbar, K. R.; Turro, C. *Inorg. Chem.* **2004**, *43*, 2450–2452.
(71) Crawford, C. A.; Matonic, J. H.; Huffman, J. C.; Folting, K.; Dunbar, K. R.; Christou, G. *Inorg. Chem.* **1997**, *36*, 2361–2371.
(72) Fees, J.; Ketterle, M.; Klein, A.; Fiedler, J.; Kaim, W. *J. Chem. Soc., Dalton Trans.* **1999**, 2595–2599; and references therein.
(73) Berger, S.; Fiedler, J.; Reinhardt, R.; Kaim, W. *Inorg. Chem.* **2004**, *43*, 1530–1538; and references therein.
(74) Waterland, M. R.; Gordon, K. C. *J. Raman Spectrosc.* **2000**, *31*, 243–253.
(75) Lundin, N. J.; Walsh, P. J.; Howell, S. L.; McGarvey, J. J.; Blackman, A. G.; Gordon, K. C. *Inorg. Chem.* **2005**, *44*, 3551–3560.
(76) Waterland, M. R.; Gordon, K. C.; McGarvey, J. J.; Jayaweera, P. M. *J. Chem. Soc., Dalton Trans.* **2006**, 609–616.
(77) Dougan, S. J.; Habtemariam, A.; McHale, S. E.; Parsons, S.; Sadler, P. J. *Proc. Nat. Acad. Sci. U.S.A.* **2008**, *105*, 11628–11633.

Experimental Section

Materials. The reagents 1,10-phenanthroline, 1,2-phenylenediamine, nitric acid, sulfuric acid and potassium bromide were purchased from Acros. The compound 1,10-phenanthroline-5,6-dione was occasionally purchased from Aldrich. Anhydrous (99.9%) DMF (*N*,*N*-dimethylformamide) was purchased from Aldrich. The reagents 4,5-dimethoxy-1,2-phenylenediamine dihydrochloride and 4,5-dichloro-1,2-phenylenediamine were obtained from Alfa-Aesar. The reagents 4,5-dimethyl-1,2-phenylenediamine and 4-cyano-*o*-phenylenediamine were purchased from TCI and Sigma-Aldrich, respectively. The starting material $RhCl_3.H_2O$ was purchased from Pressure Chemicals. The compounds $Rh_2(O_2CCH_3)_4(CH_3OH)_2$[78] and *cis*-$[Rh_2(O_2CCH_3)_2(dppz)_2](O_2CCH_3)_2$[68] (**1**) were prepared according to published procedures. The compounds 1,10-phenanthroline-5,6-dione,[79] dipyrido[3,2-*a*:2′,3′-*c*]phenazine (dppz),[79] 7,8-dimethyldipyrido[3,2-*a*:2′,3′-*c*]phenazine (Me_2dppz),[66] 7,8-dinitrodipyrido[3,2-*a*:2′,3′-*c*]phenazine ($(NO_2)_2$dppz),[80] and 7,8-dichlorodipyrido[3,2-*a*:2′,3′-*c*]phenazine (Cl_2dppz)[76] were all prepared according to published literature procedures.

Agarose, ethidium bromide, EDTA, Tris/HCl and the RNA loading solution were purchased from Sigma and used as received. The pGEM linear DNA control template (3995 bp) was purchased from Promega; the T7-RNAP enzyme (50 units/μL) and 5× RNA transcription buffer were purchased from Invitrogen. The protein marker "Precision Plus Protein Dual Color Standards" and the brilliant blue staining solution were purchased form Bio-Rad.

Syntheses of Substituted dppz Ligands and *cis*-$[Rh_2(O_2CCH_3)_2(R_1R_2dppz)_2]^{2+}$ Complexes. 7-Cyanodipyrido[3,2-*a*:2′,3′-*c*]-phenazine (CNdppz). A mixture of 1,10-phenanthroline-5,6-dione (158 mg, 0.75 mmol) and 4-cyano-*o*-phenylenediamine (100 mg, 0.75 mmol) was refluxed in ethanol (12 mL) for 3 h under nitrogen. After cooling, the yellow suspension was collected by filtration, washed with ethanol, and dried to afford a yellow solid (yield 180 mg, 78%). ESI-MS for $[CNdppz + 1]^{1+}$ *m*/*z*: 308.1. ^{1}H NMR (CD_3Cl), δ (ppm): 7.85 (q, 2H), 8.04 (dd, 1H), 8.46 (d, 1H), 8.76 (d, 1H), 9.33 (m, 2H), 9.63 (m, 2H). Calcd for $C_{19}H_9N_5$: C 74.26, N 22.79, H 2.95. Found: C 74.00, N 22.68, H 2.95.

7,8-Dimethoxydipyrido[3,2-*a*:2′,3′-*c*]phenazine ($(MeO)_2$dppz). A mixture of 1,10-phenanthroline-5,6-dione (348 mg, 1.66 mmol), 4,5-dimethoxy-1,2-phenylenediamine dihydrochloride (500 mg, 2.07 mmol), and triethylamine (12 mL) was refluxed in ethanol (30 mL) for 30 min under nitrogen. After cooling, the yellow suspension was collected by filtration, washed with ethanol, and air-dried to afford a tan solid (yield 483 mg, 85%). ESI-MS for $[(MeO)_2dppz + 1]^{1+}$ *m*/*z*: 343.2. ^{1}H NMR ($CDCl_3$), δ (ppm): 4.15 (s, 6H, MeO), 7.42 (s, 2H), 7.78 (m, 2H), 9.18 (d, 2H), 9.43 (d, 2H). Calcd for $C_{20}H_{14}N_4O_2$: C 70.17, N 16.36, H 4.12. Found: C 69.83, N 15.95, H 4.11.

Complex Syntheses. *cis*-$\{Rh_2(O_2CCH_3)_2[(MeO)_2dppz]_2\}(O_2CCH_3)_2$ (2). A solution of $Rh_2(O_2CCH_3)_4$ (161 mg, 0.36 mmol) in acetonitrile (12 mL) was treated with $(MeO)_2$dppz (250 mg, 0.73 mmol) in acetonitrile (5 ml), and the suspension was refluxed for 48 h under nitrogen. After this time period, the brown solid was collected by filtration, washed with acetonitrile, and dried in vacuo (yield 328 mg, 81%). ESI-MS for $\{Rh_2(O_2CCH_3)_2[(MeO)_2dppz]_2\}^{2+}$ *m*/*z*: 504.1. ^{1}H NMR (CD_3OD), δ (ppm): 1.70 (s, 6H, CH_3CO_2), 2.60 (s, 6H, CH_3CO_2), 4.0 (s, 12H, MeO), 7.06 (s, 4H, dppz), 7.71 (m, 4H, dppz), 8.58 (m, 4H, dppz), 8.98 (m, 4H, dppz). Calcd for $Rh_2C_{48}H_{40}N_8O_{12}\cdot 8H_2O$: C 45.36, N 8.82, H 4.44. Found: C 45.00, N 8.91, H 4.25.

***cis*-$\{Rh_2(O_2CCH_3)_2(Me_2dppz)_2\}(O_2CCH_3)_2$ (3).** A solution of $Rh_2(O_2CCH_3)_4(CH_3OH)_2$ (163 mg, 0.32 mmol) in acetonitrile (12 mL) was treated with Me_2dppz (200 mg, 0.65 mmol) in acetonitrile (5 ml), and the suspension was refluxed for 48 h under nitrogen, after which time, the brown-red solid was collected by filtration, washed with acetonitrile, and air-dried (yield 287 mg, 84%). ESI-MS for $[Rh_2(O_2CCH_3)_2(Me_2dppz)_2]^{2+}$ *m*/*z*: 472.0. ^{1}H NMR (CD_3OD), δ (ppm): 1.75 (s, 6H, CH_3CO_2), 2.58 (s, 12H, Me), 2.60 (s, 6H, CH_3CO_2), 7.43 (s, 4H, dppz), 7.71 (m, 4H, dppz), 8.60 (m, 4H, dppz), 8.93 (m, 4H, dppz). Calcd for $Rh_2C_{48}H_{40}N_8O_8\cdot 10H_2O$: C 41.39, N 8.04, H 3.62. Found: C 41.99, N 8.01, H 3.75.

***cis*-$\{Rh_2(O_2CCH_3)_2(Cl_2dppz)_2\}(O_2CCH_3)_2$ (4).** A solution of $Rh_2(O_2CCH_3)_4(CH_3OH)_2$ (72 mg, 0.14 mmol) in acetonitrile (12 mL) was treated with Cl_2dppz (100 mg, 0.28 mmol) in acetonitrile (5 ml), and the suspension was refluxed for 48 h under nitrogen. After the solution was cooled, the dark brown solid was filtered, washed with acetonitrile, and dried in vacuo (yield 156 mg, 97%). ESI-MS for $[Rh_2(O_2CCH_3)_2(Cl_2dppz)_2]^{2+}$ *m*/*z*: 512.9. ^{1}H NMR ($CDCl_3$), δ (ppm): 1.62 (s, 6H, CH_3CO_2), 1.64 (s, 6H, CH_3CO_2), 7.46 (m, 4H, dppz), 7.96 (s, 4H, dppz), 8.65 (m, 4H, dppz), 8.80 (m, 4H, dppz). Calcd for $Rh_2C_{44}H_{28}N_8O_8Cl_4\cdot CH_3OH$: C 45.94, N 9.52, H 2.74. Found: C 45.56, N 9.80, H 2.64.

***cis*-$\{Rh_2(O_2CCH_3)_2(CNdppz)_2\}(O_2CCH_3)_2$ (5).** A solution of $Rh_2(O_2CCH_3)_4$ (100 mg, 0.23 mmol) in acetonitrile (12 mL) was treated with CNdppz (139 mg, 0.45 mmol) in acetonitrile (5 ml), and the suspension was refluxed for 48 h under nitrogen. The resulting brown solid was collected by filtration, washed with acetonitrile, and dried in vacuo (yield 222 mg, 91%). ESI-MS for $[Rh_2(O_2CCH_3)_2(CNdppz)_2]^{2+}$ *m*/*z*: 469.0. ^{1}H NMR (CD_3OD), δ (ppm): 1.62 (s, 6H, CH_3CO_2), 2.60 (s, 6H, CH_3CO_2), 7.78 (m, 4H, dppz), 7.91 (d, 2H, dppz), 8.12 (m, 2H, dppz), 8.20 (d, 2H), 8.72 (m, 2H, dppz), 9.01 (m, 4H, dppz). Calcd for $Rh_2C_{46}H_{30}N_{10}O_8\cdot 3H_2O\cdot CH_3CN$: C 48.17, N 12.87, H 3.03. Found: C 47.95, N 12.30, H 3.11.

***cis*-$\{Rh_2(O_2CCH_3)_2[(NO_2)_2dppz]_2\}(O_2CCH_3)_2$ (6).** A solution of $Rh_2(O_2CCH_3)_4(CH_3OH)_2$ (68 mg, 0.13 mmol) in acetonitrile (12 mL) was treated with $(NO_2)_2$dppz (100 mg, 0.27 mmol) in acetonitrile (5 ml), and the suspension was refluxed for 48 h under nitrogen. After this time period, the dark brown/black suspension was cooled to room temperature, and the solid was collected by filtration, washed with acetonitrile, and dried to afford a dark brown product (144 mg, 93% yield). MALDI for $\{Rh_2(O_2CCH_3)_2[(NO_2)_2dppz]_2\}^{2+}$ *m*/*z*: 533.8. ^{1}H NMR (DMF-d_7, $CDCl_3$, referenced to DMF-d_7), δ (ppm): 1.89 (s, 6H, CH_3CO_2), 1.97 (s, 6H, CH_3CO_2), 7.37 (m, 4H, dppz), 8.74 (s, 4H, dppz), 9.35 (m, 4H, dppz), 9.97 (m, 4H, dppz). Calcd for $Rh_2C_{44}H_{28}N_{12}O_{16}\cdot 4H_2O\cdot CH_3CN$: C 40.63, N 13.39, H 2.59. Found: C 40.91, N 13.77, H 2.68.

Instrumentation. The ^{1}H NMR spectra were recorded on Varian 300 or 500 MHz spectrometers and were referenced to the residual proton impurities in the deuterated solvents. X-band electron paramagnetic resonance (EPR) spectra were recorded on a Bruker EMX spectrometer equipped with a Hewlett-Packard 5352B microwave frequency counter, an ER4102 ST cavity, and the Oxford Instruments ESR 900 Cryostat. The UV−visible measurements were performed with a Shimadzu UV−visible 1601PC spectrophotometer. Electrochemical measurements were carried out by using an H-CH Electrochemical Analyzer model 620A. Cyclic voltammetric measurements were performed in 99.9% dry dimethylformamide (DMF), purchased from Aldrich, with 0.2 M tetra-*n*-butyl ammonium hexafluorophosphate ($TBAPF_6$) as the supporting electro-

(78) Rempel, G. A.; Legzdins, P.; Smith, H.; Wilkinson, G. *Inorg. Synth.* **1972**, *13*, 90–91.
(79) Dickeson, J. E.; Summers, L. A. *Aust. J. Chem.* **1970**, *23*, 1023–1027.
(80) Kleineweischede, A.; Mattay, J. *J. Organomet. Chem.* **2006**, *691*, 1834–1844 and references therein.

lyte. The working electrode was a BAS Pt disk electrode, the reference electrode was Ag/AgCl (in saturated NaCl solution), and the auxiliary electrode was a Pt wire. The ethidium bromide stained agarose gels (1%) were imaged on an Alpha Imager 2000 transilluminator (Alpha Innotech Corporation).

Methods. Transcription Inhibition Experiments. The transcription assay has been previously discussed in the literature.[28−30] In the in vitro transcription experiment, the pGEM linear DNA template (120 μM bases) was used with T7-RNAP, resulting in two transcripts of length 1065 and 2346 bases; each trial was performed three times. The transcription reaction was conducted for 45 min at 37 °C (40 mM Tris/HCl pH = 8.0, 8 mM $MgCl_2$, 25 mM NaCl) in nuclease free water in the presence of 2.3 units of T7-RNAP and 1.0 mM of each ATP, CTP, GTP, and UTP (NTPs). The inhibition of mRNA production by the dirhodium compounds was detected in vitro by the measurement of the mRNA generated upon addition of increasing amounts of metal complex to the assay. The concentration of each complex at which 50% of the transcription is inhibited, IC_{50}, was calculated by interpolation of the integrated areas of the imaged mRNA signal of each lane of the gel conducted with various concentrations of a given complex. All stock solutions of the metal complexes were prepared in 1% DMSO/99% H_2O. For the experiments, the metal stock solutions were diluted by 100-fold with H_2O to make them 0.01% in DMSO. Control experiments indicated that the amount of DMSO introduced into each transcription assay does not interfere with the process. The concentration of T7-RNAP purchased from Invitrogen was determined by measuring the absorbance at 280 nm with an extinction coefficient $\varepsilon_{280} = 1.4 \times 10^5\ M^{-1}cm^{-1}$;[61,81] the T7-RNAP concentration in each well for the transcription assays was approximately 10 μM.

Non-Denaturing PAGE (Polyacrylamide Gel Electrophoresis). Electrophoretic mobility shift assays were performed by incubating T7-RNAP with the dirhodium complexes **1**−**6** under the same conditions used for the transcription inhibition assay. For this experiment, 1.5 μL of T7-RNAP solution was mixed with 3.5 μL transcription buffer and the respective dirhodium complex **1**−**6** at a concentration equal to the IC_{50} value calculated from the transcription inhibition assay (for each complex); water was added to a total volume of 15 μL. This mixture was incubated for 1 h at 37 °C. After adding 5 × loading buffer, the samples were loaded on a non-denaturing 10% polyacrylamide gel. Electrophoresis was carried out with a vertical system at 120 V for 5 h. The gel was stained with brilliant blue solution and subsequently imaged. The protein marker used was "Precision Plus Protein Dual Color Standards".

Density Functional Theory (DFT) Calculations. DFT calculations were performed on the dirhodium complexes **1**−**6** with the hybrid Becke-3 parameter exchange functional and the Lee−Yang−Parr non-local correlation functional (B3LYP) implemented in the Gaussian 98 program suite.[82−84] Geometry optimizations were carried out using the SDD basis set-relativistic effective core potential (RECP), which combines the Huzinaga−Dunning double-ζ basis set on the main group elements with the Stuttgart−Dresden basis set-RECP combination for the rhodium atoms, while for all other atoms, the 6-311G(d) basis set was employed.[85] To model the dirhodium complexes in aqueous solution, the molecules were embedded in a dielectric medium as an approximation to include solvent polarization effects. The inclusion of the dielectric medium was considered using the Tomasi's Polarized Continuum Model (PCM) reaction field model for the optimization of the molecular geometry.[86,87] All calculations were performed on an Altix 3700 128-processor SGI computer or a p575 640-processor IBM computer located in the Laboratory for Molecular Simulations at Texas A&M University.

Table 1. Electrochemical Reduction Potentials $E_{1/2(red)}$ (vs. Ag/AgCl) in Dry DMF for R_1R_2dppz Ligands

R_1R_2dppz	$E_{1/2(red)}$ (V)[a]
$(MeO)_2$dppz	−1.25
Me_2dppz	−1.14
dppz	−1.06
Cl_2dppz	−0.83
CNdppz	−0.74, −1.50
$(NO_2)_2$dppz	+0.10, −0.27

[a] The reduction potentials were measured in dry DMF with a Ag/AgCl reference electrode at 20 °C. All reduction processes are reversible.

Results

Synthesis and Characterization of the Substituted dppz Ligands and Dirhodium Complexes. Dppz and the substituted dppz ligands were synthesized as previously described,[66,76,79,80] except for CNdppz and $(MeO)_2$dppz, which are new compounds (it was not possible to synthesize $(CN)_2$dppz). Each substituted dppz ligand was synthesized by Schiff-base condensation of 1,10-phenanthroline-5,6-dione with the appropriate substituted diaminobenzene compound or the dihydrochloride salt in ethanol under refluxing conditions. The dirhodium complexes **1**−**6** were prepared by refluxing $Rh_2(O_2CCH_3)_4(CH_3OH)_2$ with the appropriate dppz ligand; the reactions involve substitution of two acetate groups on the dirhodium core by the unsubstituted/substituted dppz ligands.

Electrochemical data for the dppz ligands are listed in Table 1. As expected, substitution of positions 7,8 of dppz with electron withdrawing groups (Chart 1; Cl, CN and NO_2) results in less negative reduction potentials as compared to unsubstituted dppz, whereas electron donating groups (MeO, Me) in the same positions render the opposite effect.[66,74,75] For the investigated region in DMF, all the dppz ligands exhibit one reversible single-electron reduction process, except for CNdppz and $(NO_2)_2$dppz, which exhibit two reversible reduction processes (Table 1), in good agreement with the electron-withdrawing properties of the CN and NO_2 groups.[80] Accordingly, the ligand-based reduction potentials

(81) Gill, S. C.; von Hippel, P. H. *Anal. Biochem.* **1989**, *182*, 319–326.
(82) Frisch, M. J. ; Trucks, G. W.; Schlegel, H. B.; Scuseria, G. E.; Robb, M. A.; Cheeseman, J. R.; Zakrzewski, V. G.; Montgomery, J. A.; Stratmann, R. E.; Burant, J. C.; Dapprich, S.; Millam, J. M.; Daniels, A. D.; Kudin, K. N.; Strain, M. C.; Farkas, O.; Tomasi, J.; Barone, V.; Cossi, M.; Cammi, R.; Mennucci, B.; Pomelli, C.; Adamo, C.; Clifford, S.; Ochterski, J.; Petersson, G. A.; Ayala, P. Y.; Cui, Q.; Morokuma, K.; Malick, D. K.; Rabuck, A. D.; Raghavachari, K.; Foresman, J. B.; Cioslowski, J.; Ortiz, J. V.; Stefanov, B. B.; Liu, G.; Liashenko, A.; Piskorz, P.; Komaromi, I.; Gomperts, R.; Martin, R. L.; Fox, D. J.; Keith, T.; Al-Laham, M. A.; Peng, C. Y.; Nanayakkara, A.; Gonzalez, C.; Challacombe, M.; Gill, P. M. W.; Johnson, B. G.; Chen, W.; Wong, M. W.; Andres, J. L.; Head-Gordon, M.; Replogle, E. S.; Pople J. A. *Gaussian 98*, revision A.7; Gaussian, Inc.: Pittsburgh, PA, 1998.
(83) Becke, A. D. *J. Chem. Phys.* **1993**, *98*, 5648–5652.
(84) Lee, C.; Yang, W.; Parr, R. G. *Phys. Rev. B* **1988**, *37*, 785.
(85) Andrae, D.; Häussermann, U.; Dolg, M.; Stoll, H.; Preuss, H. *Theor. Chim. Acta* **1990**, *77*, 123–141.
(86) Cossi, M.; Barone, V.; Cammi, R.; Tomasi, J. *Chem. Phys. Lett.* **1996**, *255*, 327–335.
(87) Miertus, S.; Scrocco, E.; Tomasi, J. *Chem. Phys.* **1981**, *55*, 117–129.

Table 2. Electronic Absorption Spectral Data for R_1R_2dppz Ligands and Dirhodium Complexes

compound	λ_{max}/nm ($\varepsilon/10^4$ $M^{-1}cm^{-1}$)	solvent	ref
$(MeO)_2$dppz	280 (3.62), 379 (1.22), 400 (2.23)	CH_2Cl_2	this work
2	213 (7.96), 295 (9.0), 396 (3.75)	MeOH	this work
Me_2dppz	274 (6.11), 347 (0.75), 355 (0.945), 366 (1.39), 374 (1.22), 386 (1.82)	CH_2Cl_2	74, 76
3	210 (63.2), 285 (10.68), 380 (18.7)	MeOH	this work
dppz	269 (5.12), 343 (0.91), 351 (1.01), 360 (1.23), 368 (1.11), 379 (1.29)	CH_2Cl_2	74
1	203 (6.939), 276 (8.643), 363 (1.517), 434 (0.5459)	H_2O	68
Cl_2dppz	272 (5.39), 370 (1.54), 391 (2.13)	CH_2Cl_2	76
4	218 (3.5), 279 (6.85), 371 (1.56), 391 (1.55)	MeOH	this work
CNdppz	271 (5.86), 295 (3.79), 305 (2.7), 367 (1.7), 387 (1.8)	CH_2Cl_2	this work
5	211 (9.81), 271 (16.87), 347 (2.89)	MeOH	this work
$(NO_2)_2$dppz	228 (5.45), 233 (5.25), 249 (4.40), 293 (2.01), 304 (1.67), 389 (0.61)	CH_2Cl_2	80
6	284 (9.765), 387 (2.181)	MeOH	this work

of complexes **1**−**6** are expected to follow the same trend, namely **2** being the hardest to reduce and **6** the easiest. Complexes **1**−**6** were characterized by spectroscopic and analytical methods. The UV/vis data for the ligands from the present and previous spectroscopic studies are listed in Table 2. The absorption bands of the ligands and the complexes in the 360−370 nm region are assigned to dppz $\pi-\pi^*$ ligand centered (LC) transitions.[68,75,76] Stronger LC transitions are observed at higher energies (λ < 300 nm). Apart from the LC transitions, the complexes exhibit several broad and intense bands that may be assigned as MLCT bands.

Transcription Inhibition Studies. The inhibition of transcription by each dirhodium complex was determined by recording the imaged mRNA produced during the transcription reaction as a function of complex concentration, while keeping the concentrations of all other components constant. A typical imaged gel is shown for *cis*-$\{Rh_2(O_2CCH_3)_2(Cl_2dppz)_2\}(O_2CCH_3)_2$ (**4**) in Figure 1; the produced mRNA decreases relative to the control lane (no metal complex, lane 1) as the complex concentration increases (lanes 2−5). The concentration of each complex required to inhibit 50% of the transcription in vitro is listed in Table 3. For comparison sake, the transcription inhibition assay was conducted in the presence of increasing amounts of cisplatin and dirhodium tetraacetate. The measured IC_{50} values for cisplatin and dirhodium tetraacetate are 10.9 and 13.6 μM, respectively, under the same experimental conditions as those used for compounds **1**−**6**.

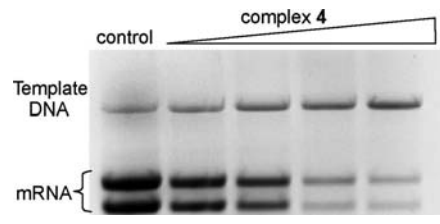

Figure 1. Ethidium bromide stained agarose gel (1%) of transcribed mRNA produced from the transcription reaction in the absence (lane 1; control) and with increasing concentrations of compound **4**: 0.5 μM (lane 2), 1 μM (lane 3), 2 μM (lane 4), and 4 μM (lane 5).

Table 3. IC_{50} (μM) Values for Compounds **1**−**6**

complex	R_1R_2dppz	IC_{50} (μM)[a]
2	$(MeO)_2$dppz	1.1
3	Me_2dppz	1.5
1	dppz	2.0
4	Cl_2dppz	2.4
5	CNdppz	2.5[b]
6	$(NO_2)_2$dppz	3.2

[a] The complex solutions were prepared in 1% DMSO/99% H_2O; the IC_{50} values recorded for cisplatin and dirhodium tetraacetate under the same experimental conditions are 10.9 and 13.6 μM, respectively. [b] If the complex is dissolved in 1% MeOH/99% H_2O, the IC_{50} value remains the same.

An assessment of the IC_{50} values for complexes **1**−**6** listed in Table 3 indicates that a higher concentration of dirhodium complex is necessary to inhibit the transcription reaction as the substituents on the dppz ligand become more electron-withdrawing. A mechanism of transcription inhibition involving binding of complexes **1**−**6** to the DNA is ruled out for several reasons. First, previous studies in our laboratories on the unsubstituted bis dppz complex *cis*-$[Rh_2(O_2CCH_3)_2(dppz)_2]^{2+}$ revealed that it cannot intercalate between the DNA bases.[68] Second, compounds **1**−**6** do not appear to react with DNA purine bases to form covalent adducts as evidenced by NMR studies, which indicated that even after refluxing compounds **1**−**6** in the presence of 9-ethylguanine for several days, there is no substitution of the acetate groups.[18−22] Finally, binding of **1**−**6** to the NTPs can be ruled out as a mechanism of transcription inhibition because each NTP is present in a large excess (1 mM) relative to the concentration of the metal complexes (<5 μM) in the transcription assays. The aforementioned observations for **1**−**6** along with the fact that dppz ligands are good electron-acceptors,[72−74] point to an alternative mechanism of transcription inhibition involving redox reactions with the cysteine residues of T7-RNA.

EPR Studies of the Radical Species of Dirhodium Complexes 1−6. It is known that cysteine thiols are important for the regulation of protein function and that reactive cysteine thiols are readily oxidized.[88,89] The reduction reactions of **1**−**6** were effected by addition of a stoichiometric quantity of cysteine in water to the dirhodium complex (typically brown solutions), producing deep blue/violet colored solutions that exhibit an intense electronic absorption at ~ 800 nm (an analogous intense blue color was previously reported for the reduced dirhodium species $[Rh_2(O_2CCH_3)_2(bpy)_2(MeCN)_2]^{+}$ [71]). The aforementioned blue solutions were immediately subjected to EPR spectroscopy (Table 4; Figures 2 and 3).

All reduced dirhodium bis-dppz complexes **1**−**6** exhibit similar EPR signals (Figures 2 and 3), which are attributed to the radical species $[Rh_2(O_2CCH_3)_2(R_1R_2dppz)_2]^{\bullet+}$ (R_1 and R_2 defined in Chart 2), with characteristic isotropic values g

(88) Sanchez, R.; Riddle, M.; Woo, J.; Momand, J. *Protein Sci.* **2008**, *17*, 473–481.
(89) Wilcox, D. E.; Schenk, A. D.; Feldman, B. M.; Xu, Y. In *Antioxidants and Redox Signaling*; Mary Ann Liebert, Inc.: Larchmont, NY, 2001; Vol. 3 (4), pp 549−564.

Table 4. EPR Data for Radical Forms of **1**−**6** in Frozen DMSO/H_2O Solutions at 10 K

Complex	Radical form[a]	g	ΔH^b(mT)
2	$\{Rh_2(O_2CCH_3)_2[(MeO)_2dppz]_2\}^{\bullet+}$	2.003	2.7
3	$[Rh_2(O_2CCH_3)_2(Me_2dppz)_2]^{\bullet+}$	2.003	2.7
1	$[Rh_2(O_2CCH_3)_2(dppz)_2]^{\bullet+}$	2.003	4.5
4	$[Rh_2(O_2CCH_3)_2(Cl_2dppz)_2]^{\bullet+}$	2.003	1.6
5	$[Rh_2(O_2CCH_3)_2(CNdppz)_2]^{\bullet+}$	2.003	1.3
6	$\{Rh_2(O_2CCH_3)_2[(NO_2)_2dppz]_2\}^{\bullet+}$	2.003	1.7

[a] Radical forms generated by reaction of each compound with cysteine. [b] Peak-to-peak line width.

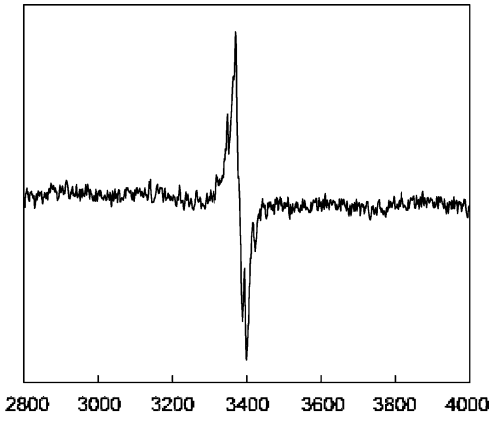

Figure 2. EPR spectrum of the $\{Rh_2(O_2CCH_3)_2[(MeO)_2dppz]_2\}^{\bullet+}$ radical in frozen DMSO/H_2O solution at 10 K.

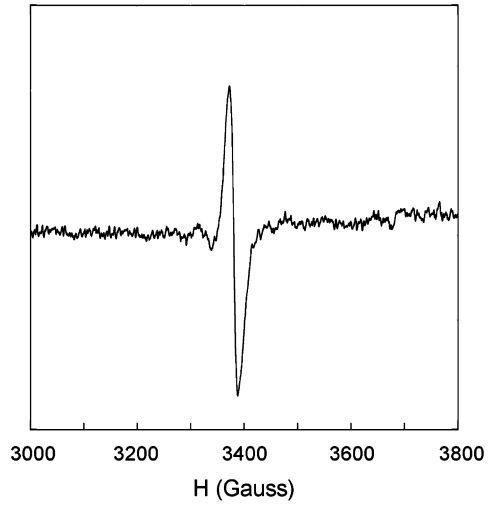

Figure 3. EPR spectrum of the $[Rh_2(O_2CCH_3)_2(Cl_2dppz)_2]^{\bullet+}$ radical in frozen DMSO/H_2O solution at 10 K.

$= 2.003$. The g values for the dirhodium complex radicals (Table 4) are essentially identical to the reported g values for the free dppz radical anions ($g \sim 2.0032$),[72,73,90] which suggests that the unpaired electron is delocalized in the b_1(phz) orbital as noted for other dppz transition metal complexes.[73] The EPR spectra of **1**−**6** (e.g., Figures 2 and 3) are isotropic, unlike the axial or rhombic spectra observed for reduced Rh_2^{3+} species in which the unpaired electron is located in a metal-based orbital such as the σ^* molecular orbital.[91−93] A ligand-based EPR spectrum with $g \sim 2.0$ was previously reported for a related dirhodium diimine complex, namely $[Rh_2(O_2CCH_3)_2(bpy)_2(MeCN)_2](BF_4)$.[71] In the case of the radical form of **2**, $\{Rh_2(O_2CCH_3)_2[(MeO)_2dppz]_2\}^{\bullet+}$ (Figure 2; $a(^{14}N) \sim 1.7$ mT), and to a lesser extent the radical of **1** and **3**, the ^{14}N ($I = 1$) hyperfine splitting is observed as a quintet (1:2:3:2:1) because of coupling of the unpaired electron with the two equivalent phz nitrogen atoms.[72,90] The *a*-diimine ^{14}N coupling constants are generally smaller than those for phz and were not detected in the reduced forms of **1**−**3**, thus confirming the b_1(phz) character of the singly occupied orbital localized at the phz moiety of the molecule. No hyperfine coupling to ^{103}Rh ($I = 1/2$; ^{103}Rh isotropic hyperfine constant $a_0 = 43.85$ mT [94]) was detected in any case, but the breadth of the signals (Table 4) indicates a marginal Fermi contact term for heavy-metal nuclei centers, which induce rapid relaxation.[72,90] In the cases of the radical species of **4**−**6** with the electron-withdrawing ligands Cl (Figure 3), CN, and NO_2, respectively, the EPR spectra are isotropic with values $g \sim 2.003$ (Table 4) with no hyperfine splitting being observed. The aforementioned characteristics of the EPR spectra strongly support ligand-based lowest unoccupied molecular orbitals (LUMOs) for **4**−**6**, whereas the broader nature of the signals ($\Delta H > 1$ mT; Table 4) indicates more delocalized radical species on the dppz moieties.[95] The absence of hyperfine splitting because of coupling of the unpaired electron with the phz nitrogen atoms for radicals of **4**−**6** indicates that the unpaired electron is further delocalized onto the substituted end of the phz ring because of the electron-withdrawing effect of the Cl, CN, and NO_2 groups. These observations are consistent with the ^1H NMR spectra of the reduced species for **4**−**6**, which exhibit increased line widths and complete loss of the spin−spin coupling for the proton resonances, especially in the case of **6**.

PAGE (Polyacrylamide Gel Electrophoresis). Formation of disulfide bonds in T7-RNAP after incubation with the dirhodium complexes at a concentration equal to the IC_{50} for each complex, at 37 °C for 1 h, was evaluated by polyacrylamide gel electrophoresis under non-reducing conditions. For example, in Figure 4, T7-RNAP that has been incubated in the presence of **1** (lane 3) and **2** (lane 5) migrates slightly more slowly as compared to the native enzyme (lane 2). Migration on the PAGE gel is sensitive to modifications in the conformation of the protein. In this case, formation of intraprotein disulfide bonds (and other oxidized related species such as sulfenic (SOH)/sulfinic (SO_2H) acids, disulfide S-oxide) between proximal cysteine thiol groups[88,89] leads to T7-RNAP modified derivatives that migrate slightly slower on the gel than the reduced enzyme.[51] Additionally, at the top of lanes 3 and 5, two new bands appear at higher molecular weights than T7-RNAP. These bands (>250 kDa)

(90) Fees, J.; Kaim, W.; Moscherosch, M.; Matheis, W.; Klíma, J.; Krejcík, M.; Zális, S. *Inorg. Chem.* **1993**, *32*, 166–174.
(91) Le, J. C.; Chavan, M. Y.; Chau, L. K.; Bear, J. L.; Kadish, K. M. *J. Am. Chem. Soc.* **1985**, *107*, 7195–7197.
(92) Prater, M. E.; Pence, L. E.; Clérac, R.; Finniss, G. M.; Campana, C.; Auban-Senzier, P.; Jérome, D.; Canadell, E.; Dunbar, K. R. *J. Am. Chem. Soc.* **1999**, *121*, 8005–8016.
(93) Boyd, D. C.; Connelly, N. G.; Herbosa, G. G.; Hill, M. G.; Mann, K. R.; Mealli, C.; Orpen, A. G.; Richardson, K. E.; Rieger, P. H. *Inorg. Chem.* **1994**, *33*, 960–971.
(94) Kaim, W.; Berger, S.; Greulich, S.; Reinhardt, R.; Fiedler, J. *J. Organomet. Chem.* **1999**, *582*, 153–159.
(95) Bear, J. L.; Chau, L. K.; Chavan, M. Y.; Lefoulon, F.; Thummel, R. P.; Kadish, K. M. *Inorg. Chem.* **1986**, *25*, 1514–1516.

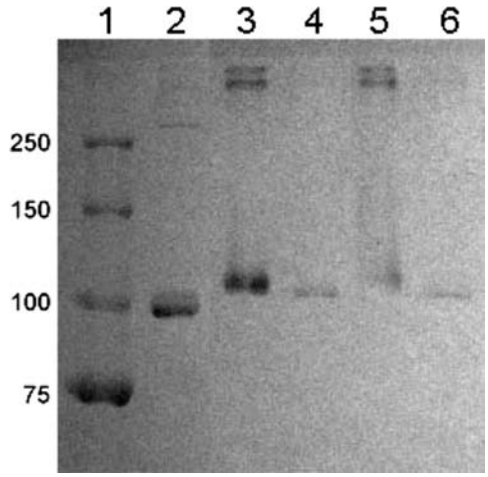

Figure 4. PAGE non-denaturing gel; Protein marker (lane 1; labeled on the side in kDa); T7-RNAP incubated at 37 °C (lane 2); T7-RNAP incubated at 37 °C in the presence of **1** (lane 3); T7-RNAP incubated at 37 °C in the presence of **1** followed by addition of DTT (dithiothreitol) (lane 4); T7-RNAP incubated at 37 °C in the presence of **2** (lane 5); T7-RNAP incubated at 37 °C in the presence of **2** followed by addition of DTT (lane 6).

Table 5. Relative Energies (eV) of LUMO/HOMO Orbitals and Metal Orbital Contribution to the HOMO's and LUMO's of **1**−**6**

complex	L	LUMO (%)	HOMO (%)	E_{LUMO} (eV)	E_{HOMO} (eV)
2	$(MeO)_2$dppz	4.3	6.7	−2.78	−6.26
3	Me_2dppz	1.7	0.40	−2.91	−6.61
1	dppz	1.2	74.8	−2.97	−6.72
4	Cl_2dppz	0.60	73.8	−3.18	−6.75
5	CNdppz	0.60,[a] 0.60[b]	79.7,[a] 79.8[b]	−3.26[c]	−6.80[c]
6	$(NO_2)_2$dppz	0.40	82.4	−3.56	−6.86

[a] Calculated for *anti* isomer. [b] Calculated for *syn* isomer. [c] *syn* and *anti* isomers have the same orbital energy.

are attributed to enzyme trimers or tetramers connected by interprotein disulfide bonds involving the cysteine thiol groups on the surface of T7-RNAP.[88] Upon addition of dithiothreitol (DTT; a strong sulfhydryl reducing agent typically used to preserve the activity of the enzyme[62]) with the loading buffer to the incubated reaction solutions of the dirhodium bis-dppz compounds (lanes 4 and 6), the interstrand disulfide cross-links responsible for the higher molecular weight bands of the T7-RNAP are no longer present which indicates that the interstrand disulfide linkages are completely cleaved (reduced), whereas the oxidation products in the bands close to the 100 kDa marker are partially reversed. Similar results for the PAGE gels were recorded for **3**−**6**. These findings indicate that the oxidation products formed between T7-RNAP and complexes **1**−**6** are partially or completely reversible.

Density Functional Theory (DFT) Calculations. Electronic structure calculations were conducted on the cations $[Rh_2(O_2CCH_3)_2(R_1R_2dppz)_2]^{2+}$ (R_1 and R_2 defined in Chart 2) to assess the effect of the R_1R_2 groups of the dppz ligands on the molecular orbital pictures of **1**−**6** and understand the properties of their reduced species. As indicated from the results in Table 5 and visualized from the orbitals depicted in Figure 5, in general, all the complexes possess LUMOs that are primarily of ligand (dppz) character (>95%), with **1**−**3** having a slightly higher metal contribution as compared to **4**−**6** which possess electron-withdrawing substitutents on the dppz ligand (Table 5). In particular, it is obvious that

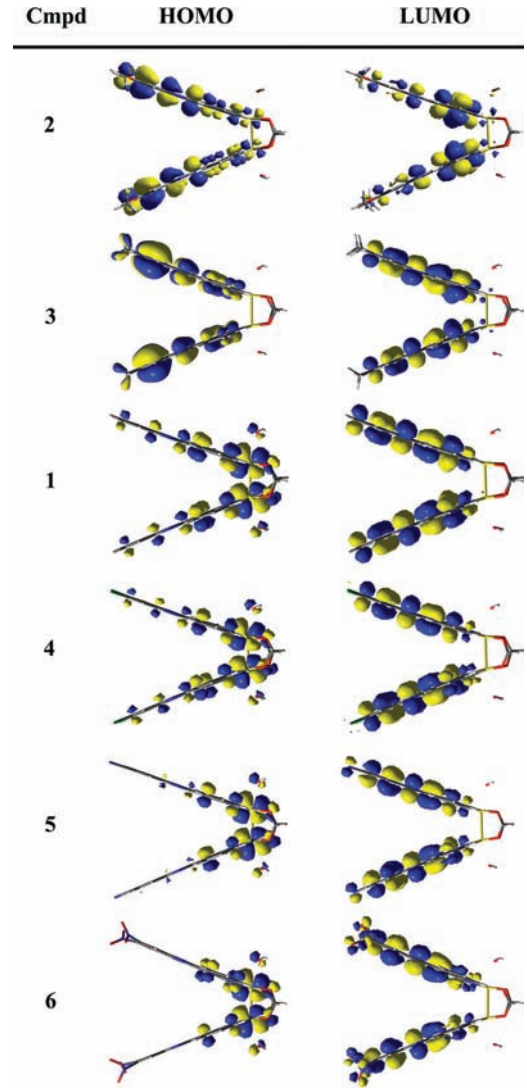

Figure 5. HOMO and LUMO Orbitals for compounds **1**−**6** depicted at 0.02 isodensity value.

Table 6. Phenazine Orbital Contribution to the LUMOs of Complexes **1**−**6**

complex	L	Phz (%)
2	$(MeO)_2$dppz	51.3
3	Me_2dppz	75.9
1	dppz	80.7
4	Cl_2dppz	87.2
5	CNdppz	87.8,[a] 69.5[b]
6	$(NO_2)_2$dppz	90.8

[a] Calculated for the *anti* isomer. [b] Calculated for the *syn* isomer.

the LUMOs of the complexes are phz-centered with the % phz contribution increasing as the electron-donating character of the dppz-substituents decreases (Table 6). Moreover, the energies of the dppz-centered LUMOs of **1**−**6** (Table 5) decrease with the electron-withdrawing character of the dppz substituents (MeO < Me < H < Cl < CN < NO_2), and this is consistent with more positive reduction potentials for R_1R_2dppz in the same order (Table 1).

Discussion

The aforementioned results support the conclusion that compounds **1**−**6** constitute a series of easily reduced

dirhodium/dppz compounds (with ligand-centered reductions) that readily oxidize cysteine and engage in redox-based reactions with T7-RNAP. The progressively increasing electron-withdrawing character of the substituents at positions 7,8 of the dppz ring for the series R_1R_2dppz (MeO < Me < H < Cl < CN < NO_2) results in more positive reduction potentials (Table 1)[74,75] and decreasing energies for the dppz-centered LUMOs of the complexes (Table 5). It is well established that for complexes with ligand-based reductions, binding of the metal centers shifts the reductions to more positive potentials;[76,77] for the present case the ordering is **2** < **3** < **1** < **4** < **5** < **6** for the ease of reduction. The ligand-centered reductions of **1**−**6** are supported by the results of the electronic structure calculations, which revealed that the complexes contain dppz-based LUMOs (Table 5) that are primarily phz in character (Chart 1b, Table 6, Figure 5). The DFT calculations are nicely corroborated by the EPR data (Figures 2 and 3) which showed that reduction of complexes **1**−**6** with cysteine leads to the formation of the radical forms $[Rh_2(O_2CCH_3)_2(R_1R_2dppz)_2]^{\bullet+}$ with isotropic values $g \sim 2.003$ akin to those reported for the free radical dppz anions (Table 4); the g values indicate an absence of spin−orbit coupling because of involvement of the Rh centers[90] and localization of the unpaired electron in the dppz portion of the reduced complexes; this conclusion is further supported by a complete absence of rhodium hyperfine coupling due to ^{103}Rh ($I = 1/2$) in the EPR spectra. The dominant phz character of the LUMOs for the complexes (Table 6; Figure 5) is supported by the EPR spectra which, in the case of $\{Rh_2(O_2CCH_3)_2[(MeO)_2dppz]_2\}^{\bullet+}$ (Figure 2) and to a lesser degree for $[Rh_2(O_2CCH_3)_2(dppz)_2]^{\bullet+}$ and $[Rh_2(O_2CCH_3)_2(Me_2dppz)_2]^{\bullet+}$, display ^{14}N ($I = 1$) hyperfine splitting due to coupling of the unpaired electron with the two equivalent phz nitrogen atoms. Independent studies of dppz and its complexes (e.g., Ru^{2+})[90] have also shown that the species possess LUMOs that are phz(b_1) in character.[72−74] In the case of the radicals of **4**−**6**, the unpaired electron is also located in a ligand-based LUMO (Table 5) with a high degree of phz character (Chart 1b, Table 6), but, as the molecular orbitals indicate (Figure 5), there is greater orbital participation from the end ring of dppz; hence, the electron is further delocalized onto the substituted part of the phz ring. This is not unexpected given the electron-withdrawing effect of the Cl, CN, and NO_2 groups. The ramification of these electronic effects is a loss of the hyperfine splitting of the unpaired electron due to the phz nitrogen nuclei (Figure 3). Apart from the delocalization of the unpaired electron onto the dppz ligand, another likely contributing factor to the breadth of the EPR signals for the radical species **4**−**6** is "electron-hopping" between dppz and $dppz^{\bullet-}$ on the time scale of the EPR experiment; this has been proposed for other homoleptic ruthenium diimine complexes.[90,96]

Apart from EPR spectroscopy, the reduction products of **1**−**6** with cysteine were also monitored by mass spectrometry. In a typical experiment, for example, the acquisition of the ESI-MS spectrum for the reaction of $[Rh_2(O_2CCH_3)_2(Me_2dppz)_2]^{2+}$ with cysteine reveals a mass peak at m/z 1064 corresponding to $[Rh_2(O_2CCH_3)_2(Me_2dppz)_2(Cys) + 1]^+$ (analogous mass peaks were detected for the other complexes in the study). The appearance of the aforementioned mass peak combined with the EPR results, suggest that the reaction proceeds by formation of a dirhodium axial adduct with the cysteine thiol, followed by transfer of the electron to the dirhodium species to form the radical species $[Rh_2(O_2CCH_3)_2(Me_2dppz)_2]^{\bullet+}$, the release of the thiyl radical ($RS^{\bullet}$) and its eventual coupling with another thiyl radical to form the cysteine disulfide product (RS-RS).[89,97] It should be pointed out, however, that the thiol oxidation may also take place in two steps through oxidation to the sulfenic acid (S-OH) or the disulfide S-oxide.[88,89,97]

In light of the aforementioned findings and previous studies indicating that complexes of the type *cis*-$[Rh_2(O_2CCH_3)_2(dppz)_2]^{2+}$ do not intercalate between the DNA bases,[68] and the much higher observed IC_{50} values for transcription inhibition by dirhodium tetraacetate as compared to **1**−**6** (Table 3), the interaction of the dirhodium dppz complexes **1**−**6** with T7-RNAP is postulated to involve redox chemistry with the cysteine thiol groups of the enzyme. It has been established that several sulfhydryl groups are vital for the activity of the T7-RNAP and that mutation of 5 out of the 12 cysteine residues results in loss of the T7-RNAP activity.[59−64] Additionally, exposure of the native enzyme to reagents that react with the accessible sulfhydryl groups such as iodoacetamide,[63] Ellman's reagent,[63] or *p*-hydroxymercuribenzoate[62] results in complete inactivation of the T7-RNAP. In this respect, the interaction of **1**−**6** with T7-RNAP was probed by (1) running the transcription assay in the presence of the complexes and, on the other hand, (2) performing the PAGE mobility shift gel assay (Figure 4) of T7-RNAP solutions subjected to complex concentrations equal to the determined IC_{50} values from the transcription assay (Table 3). It has been determined that the susceptibility of the protein cysteine thiol groups to oxidation strongly depends on the distance of the thiol group to the nearest cysteine thiol group (distances ≤6.2 Å increase the probability of disulfide bond formation), the degree of solvent exposure of the thiol groups, and the pK_a of the thiol group which depends on its local charge environment (pK_a < 9 render the groups good candidates for oxidation; for most protein thiol groups p$K_a \sim 8.5$).[88]

In the present study of T7-RNAP activity, several factors render the thiol groups particularly sensitive to redox reactions during the transcription assay including the presence of the easily reduced complexes **1**−**6** and the fact that the pH is ∼8 during the assay which induces ionization of the thiol moieties to the thiolate anions thus rendering them more reactive. The X-ray crystallographic studies of the initiation (IC)[55] and promoter[54] complexes reveal that two sets of thiol groups from the T7-RNAP cysteine residues are at distances ≤6.2 Å, which makes them susceptible to intraprotein disulfide bond formation. In particular, the distances between Cys510-Cys467, Cys515-Cys492 in the initiation and promoter complexes are 5.20, 5.71[55] and 5.14,

(96) Kaim, W.; Ernst, S.; Kasack, V. *J. Am. Chem. Soc.* **1990**, *112*, 173–178.

(97) Jourd'heuil, D.; Jourd'heuil, F. L.; Feelisch, M. *J. Biol. Chem.* **2003**, *278*, 15720–15726.

5.11 Å,[54] respectively. Moreover, it has been demonstrated by Sousa et al., that Cys467 and Cys492 are among the five T7-RNAP cysteine residues that lead to loss of enzyme activity upon mutation to serine,[59] an indication that these two residues are critical for the transcription inhibition activity. For the dirhodium species under investigation, the formation of intraprotein disulfide bonds in T7-RNAP in the presence of complexes **1** (lane 3) or **2** (lane 5) is supported by the slightly slower migration of the modified enzyme band (at ~ 100 kDa) on the PAGE gel as compared to the reduced native enzyme (Figure 4). The partial restoration of the bands at the position for the native enzyme in the presence of DTT (Figure 4; lanes 4 and 6) confirms the reversible nature of the oxidized species.

It is also important to point out that the high concentration of T7-RNAP (~ 10 μM) during the biochemical assays and the presence of several cysteine thiol groups on the surface of the protein[59] render the formation of interprotein disulfide bonds in the presence of the dirhodium complexes highly likely as well; the presence of intermolecular bonds is evidenced by the high molecular weight bands (>250 kDa) in lanes 3 and 5 (Figure 4) of the mobility shift gel, as well as their complete reversibility upon addition of DTT (lanes 4 and 6) which are attributed to enzyme trimers or tetramers connected with disulfide bonds between the exposed cysteine thiol groups on the surface of T7-RNAP.[88] Obviously, apart from the factors inherent to T7-RNAP that influence the cysteine thiol reactivity, the concentration and the properties of the oxidant have an important impact on the outcome of the reaction, as cysteinyl thiols can undergo a diverse array of redox reactions to sulfenic (S-OH)/sulfinic (SO_2H) acids, disulfide S-oxide and others.[88,89] In the case of the series of complexes **1**−**6**, the increasing electron-withdrawing character of the substituents at positions 7,8 of the dppz ring (MeO < Me < H < Cl < CN < NO_2) results in more reactive oxidizing agents in the order **2** < **3** < **1** < **4** < **5** < **6** (Table 1). The latter three complexes **4**−**6**, with the electron withdrawing groups on the dppz are expected to be more reactive toward a larger number of redox-active sites, such as all the exposed cysteine groups[59] on T7-RNAP (because of their more positive reduction potentials and their ease of reduction; vide infra). Indeed, the progressively increasing IC_{50} values in the order **2** < **3** < **1** < **4** < **5** < **6** (Table 3) suggest that the more reactive members of the series oxidize thiol groups that most likely are not critical for the activity of T7-RNAP[59] and thus a larger amount of complex is necessary to inhibit the transcription process. Despite the increased reactivity of **4**−**6**, however, the determined IC_{50} values are much lower than that of dirhodium tetraacetate (13.6 μM; Table 3) and other related complexes[28,29] which most likely form irreversible covalent adducts with T7-RNAP.

Conclusions

In the present study, the combined results of electrochemical, spectroscopic, computational, and biochemical experiments have established that the dirhodium complexes *cis*-$[Rh_2(O_2CCH_3)_2(R_1R_2dppz)_2]^{2+}$ (R_1R_2dppz = substituted dppz, Chart 2) constitute a sensitive redox-regulated series of T7-RNAP inhibitors that are readily tuned by alternating the electron-withdrawing or -donating ability of the dppz substituents the result of which is a change in the ease of the complex reduction and ultimately the extent of reactivity with the accessible T7-RNAP thiol groups. The process of transcription is inhibited in vitro by small amounts of **1**−**6** via formation of intra- and interprotein disulfide bonds that affect the critical sulfhydryl cysteine groups of the T7-RNAP. The reactivity of **1**−**6** with the reducing agent cysteine was monitored by EPR spectroscopy which revealed the formation of the radical species $[Rh_2(O_2CCH_3)_2(R_1R_2dppz)_2]^{\bullet+}$ with isotropic $g \sim 2.003$ akin to that of the free radical dppz anions. The g values of the radical species, as well as the absence of rhodium hyperfine interactions in the EPR spectra, indicate localization of the unpaired electron onto the dppz orbitals of the reduced complexes. The dominant phz character of the LUMOs for the complexes **1**−**6** was nicely corroborated by electronic structure calculations, which indicate that the unpaired electron is completely delocalized in the phz orbitals in the case of **4**−**6** with the electron withdrawing substituents on the dppz ligands. The high sensitivity of these dirhodium complexes to ligand effects and the demonstrated potential for tuning their redox activity toward T7-RNAP render them promising candidates for the control or inhibition of other important biochemical processes.

Acknowledgment. Dr. Lisa Pérez is gratefully acknowledged for assistance with the Density Functional Theory (DFT) calculations; the Laboratory for Molecular Simulations at Texas A&M University is acknowledged for providing software and computer time. The NMR instrumentation in the Chemistry Department at Texas A&M University was funded by NSF (CHE-0077917). K.R.D. thanks the Welch Foundation (A-1449) for financial support. The use of the TAMU/LBMS-Applications Laboratory (Laboratory of Biological Mass Spectroscopy) and the EPR Laboratory (Mrs. J. G. Morales and Mr. Ren Miao) are also acknowledged.

IC900164J